Atmos. Meas. Tech. Discuss., https://doi.org/10.5194/amt-2017-190
Manuscript under review for journal Atmos. Meas. Tech.
Discussion started: 27 July 2017


Atmospheric Measurement Techniques
Open Access
Discussions

# Fluctuations of radio occultation signals in sounding the Earth's atmosphere

Valery Kan[1], Michael E. Gorbunov[1], and Viktoria F. Sofieva[2]

[1]A.M.Obukhov Institute of Atmospheric Physics Russian Academy of Sciences, 119017, Moscow, Pyzhevsky per. 3
[2]Finnish Meteorological Institute, Erik Palménin aukio 1, FI-00560, Helsinki, Finnland

*Correspondence to:* Michael Gorbunov (gorbunov@ifaran.ru)

**Abstract.** We discuss the relationships that link the observed fluctuation spectra of the amplitude and phase of signals used for the radio occultation sounding of the Earth's atmosphere, with the spectra of atmospheric inhomogeneities. Our analysis employs the approximation of the phase screen and of weak fluctuations. We make our estimates for the following characteristic inhomogeneity types: 1) the isotropic Kolmogorov turbulence and 2) the anisotropic saturated internal gravity waves. We obtain the expressions for the variances of the amplitude and phase fluctuations of radio occultation signals, as well as their estimates for the typical parameters of inhomogeneity models. From the GPS/MET observations, we evaluate the spectra of the amplitude and phase fluctuations in the altitude interval from 4 to 25 $\mathrm{km}$ in the middle and polar latitudes. As indicated by theoretical and experimental estimates, the main contribution into the radio signal fluctuations comes from the internal gravity waves. The influence of the Kolmogorov turbulence is negligible. We derive simple relationships that link the parameters of internal gravity waves and the statistical characteristics of the radio signal fluctuations. These results may serve as the basis for the global monitoring of the wave activity in the stratosphere and upper troposphere.

## 1 Introduction

The regular radio occultation (RO) monitoring of the Earth's atmosphere was for the first time implemented with the aid of the low Earth orbiter (LEO) Microlab-1, which was equipped with a receiver of high-stable GPS signal at wavelengths of $\lambda_1 = 19.03\ \mathrm{cm}$ and $\lambda_2 = 24.42\ \mathrm{cm}$ at a sampling rate of 50 Hz (Ware et al., 1996). In processing RO observations, neutral atmospheric meteorological variables are retrieved from amplitude and phase measurements (Gorbunov and Lauritsen, 2004; Gorbunov et al., 2005; Gorbunov and Lauritsen, 2006), while the ionospheric contribution is removed by using the double-frequency linear combination at the same ray impact height (Vorob'ev and Krasil'nikova, 1994; Gorbunov, 2002). The impressive success of the GPS/MET experiment stimulate further development of RO satellites and constellations, including CHAMP and COSMIC experiments. Currently, the RO sounding is an important method of monitoring meteorological parameters of the Earth's atmosphere; RO data are assimilated by the world's leading numerical weather prediction centers (Rocken et al., 2000; Yunck et al., 2000; Steiner et al., 2001; Pingel and Rhodin, 2009; Poli et al., 2009; Cucurull, 2010; Poli et al., 2010; Rennie, 2010).

A high potential of the stable GPS signals, complemented with its global covering and high vertical resolution, attract the attention of researchers to the use of RO data not only for the retrieval of regular profiles, but also for the study of the inhomogeneities of the atmospheric refractivity from RO signal fluctuations (Belloul and Hauchecorne, 1997; Gurvich et al., 2000; Tsuda et al., 2000; Wang and Alexander, 2010; Cornman et al., 2004, 2012; Shume and Ao, 2016; Gubenko et al., 2008, 2011). Occultation-based methods of sounding atmospheric inhomogeneities have a long and successful history. Initially, they were used for sounding the atmospheres of other planets of the Solar system, using occultations of stars and artificial satellites (Yakovlev et al., 1974; Woo et al., 1980; Hubbard et al., 1988). For the Earth's atmosphere, occultation observations of stellar scintillations were performed at the orbital station Mir (Alexandrov et al., 1990; Gurvich et al., 2001a, b; Gurvich and Kan, 2003a, b). The observations of stellar scintillations indicated that the Earth's atmosphere is characterized by the following two types of inhomogeneities: 1) isotropic fluctuations and 2) strongly anisotropic layered structures. On the basis of these data, an empiric two-component model of 3D inhomogeneity spectrum was developed, the anisotropic component being described by the model of saturated internal gravity waves (IGW), the isotropic component being modeled as the Kolmogorov turbulence (Gurvich and Brekhovskikh, 2001; Gurvich and Kan, 2003a, b). The method of the retrieval of these parameters from the observations of stellar scintillations was successfully employed for the interpretation of the experimental data acquired at the Mir station. This method was further enhanced and applied for the bulk retrieval of IGW and turbulence parameters from the observations made by fast photometers at the GOMOS/ENVISAT satellite (Sofieva et al., 2007a). The retrievals are performed in the altitude range from 50–60 $\mathrm{km}$ down to 30 $\mathrm{km}$ (Sofieva et al., 2007b). The upper limit was determined by the radiation shot noise, the lower limit was determined by the applicability condition of the Rytov weak fluctuation theory.

In the radio band, the amplitude fluctuations are much smaller than in the optical band, therefore, the weak fluctuation theory may be applicable down to altitudes of several kilometers. The main limitation is due to the humidity fluctuations, whose role becomes significant in the troposphere. The upper boundary of the measurable fluctuation of RO signals is about 30–35 $\mathrm{km}$, which is determined mostly by residual ionospheric fluctuations and measurement noise. Optical and radio monitoring of atmospheric inhomogeneities complement each other in the regard of their height ranges. For the optical band, stratospheric IGW and turbulence make approximately equal contributions intensity fluctuations (Gurvich and Kan, 2003a, b; Sofieva et al., 2007b). For longer waves, in the radio band, a prevailing role is played by inhomogeneities, whose spectra are characterized by a steeper decrease; in our case, these are saturated IGW. Nowadays, an increasing number of papers discuss the use of GPS for the study of atmospheric inhomogeneities. Some papers link the fluctuations of the amplitude and the phase of radio signals in the stratosphere to IGWs (Tsuda et al., 2000; Steiner and Kirchengast, 2000; Wang and Alexander, 2010; Khaykin et al., 2015), while other papers attribute this part to isotropic turbulence in the lower stratosphere and troposphere (Cornman et al., 2004, 2012; Shume and Ao, 2016). Therefore, it is necessary to formulate clear criteria for determining what type of inhomogeneities, isotropic or anisotropic, dominate in radio signal fluctuations.

The aim of this paper is the clarification of the role of the two inhomogeneity types, and the evaluation of their actual contributions in the amplitude and phase of RO signals. Our analysis is based on the phase screen approximation and the weak fluctuation theory. In the framework of these approximations, we obtain simple analytical relationships for the variance of fluctuations of radio signals for anisotropic and isotropic inhomogeneities. At this stage of our study, we confined the analysis

Atmos. Meas. Tech. Discuss., https://doi.org/10.5194/amt-2017-190
Manuscript under review for journal Atmos. Meas. Tech.
Discussion started: 27 July 2017


of experimental data to height range from 25 down to 4 $\mathrm{km}$ in the middle and polar latitudes, in order to exclude the influence of complicated and volatile structure of lower-tropospheric humidity. The paper is organized as follows. In Section 2, we consider the basic models and approximations: the 3D models of anisotropic and isotropic atmospheric inhomogeneities, the phase screen approximation and the weak fluctuation theory. In Section 3, we apply these approximations to derive simple relationships for the statistical characteristics of RO signal fluctuations. In Section 4, we consider the experimental variances and fluctuation spectra of the amplitude and phase for the lower stratosphere and upper troposphere. In Section 5, we discuss the relative contribution into RO signal fluctuations coming from isotropic and anisotropic inhomogeneities. In Section 6, we offer our conclusions.

## 2 Basic Models and Approximation

For RO signal analysis, we employ the following approximations:

1) a two-component model of the 3D spectrum of the atmospheric refractivity fluctuations;

2) the approximation of the equivalent phase screen;

3) the first order approximation of the weak fluctuation theory (the Rytov approximation).

### 2.1 3D Models of Refractivity Fluctuation Spectra

For the description of the wave propagation, we define the characteristics of the random media by its 3D spectrum of the relative fluctuations of refractivity $\nu = \left(N - \bar{N}\right)/\bar{N}$, where $N = n - 1$, $n$ is the refractive index, and the overbar denotes the statistical average. We assume the regular atmosphere, $\bar{N}$, to be locally spherically symmetric. In the optics, refractivity fluctuations depend only on temperature fluctuations. In the radio range, humidity fluctuations make an additional contribution into refractivity fluctuations, which may be crucial in the lower troposphere (Eaton et al., 1988).

Stellar occultations indicated that the atmosphere is characterized by two types of density fluctuations: 1) large-scale anisotropic ones and 2) isotropic ones (Gurvich and Kan, 2003a, b; Sofieva et al., 2007a). Based on these observations, Gurvich developed a 3D model of the spectrum of relative fluctuations of refractivity, which includes two statistically-independent components: 1) anisotropic fluctuations $\Phi_W$ and 2) isotropic fluctuations $\Phi_K$ (Gurvich and Brekhovskikh, 2001; Gurvich and Kan, 2003a, b):

$$\Phi_\nu\left(\boldsymbol{\kappa}\right) = \Phi_W\left(\boldsymbol{\kappa}\right) + \Phi_K\left(\kappa\right) \tag{1}$$

where $\boldsymbol{\kappa}$ is the 3D wave number. It is assumed that the random field $\nu$ is locally homogeneous in a spherical layer. This allows taking the anisotropy of refractivity irregularities into account (Gurvich, 1984; Gurvich and Brekhovskikh, 2001).

Atmos. Meas. Tech. Discuss., https://doi.org/10.5194/amt-2017-190
Manuscript under review for journal Atmos. Meas. Tech.
Discussion started: 27 July 2017


Atmospheric Measurement Techniques Discussions

Both components of the spectrum have a power law interval with the power of $-\mu$, which is confined between the outer scale $L_{W,K}$ and the inner scale $l_{W,K}$ of the inhomogeneities. Both components can be expressed in the following general form:

$$\Phi = \Phi_{W,K} = AC^2_{W,K}\eta^2\left(\kappa_z^2+\eta^2\kappa_\perp^2+K^2_{W,K}\right)^{-\mu/2}\phi\left(\frac{\kappa}{\kappa_{W,K}}\right),$$
$$\kappa^2=\kappa_z^2+\eta^2\kappa_\perp^2,\quad \kappa_\perp^2=\kappa_x^2+\kappa_y^2 \tag{2}$$

where $C^2_{W,K}$ are the structure constants determining the fluctuation intensity $\nu$, $\eta\geq 1$ is the anisotropy coefficient characterized the ratio of the characteristic horizontal and vertical scales, $\kappa_z$ is the vertical wavenumber, $\kappa_x$, $\kappa_y$ are the horizontal wavenumbers, the direction of axis $x$ coincides with that of the incident ray, $K_{W,K}=2\pi/L_{W,K}$ and $k_{W,K}=2\pi/l_{W,K}$ are the outer and inner scale, respectively. Function $\phi$ determines the damping of the spectrum for the smallest scales. We will use the following function: $\phi=\exp\left(-\kappa^2/\kappa^2_{W,K}\right)$.

For $\mu=5$, $\eta\gg 1$, $A=1$ the spectrum (2) $\Phi=\Phi_W$ is a 3D generalization of the known model of saturated IGWs with the vertical 1D spectrum with the slope $-3$ (Smith et al., 1987; Fritts, 1989). We will use a model of the IGW spectrum with a constant anisotropy $\eta=\mathrm{const}\gg 1$, although the latest studies of stellar scintillations (Kan et al., 2012, 2014) indicate that the anisotropy increases and saturates with increasing scale; the saturation value being about 100 for vertical scales of about 100 $\mathrm{m}$. Below, we will see that the characteristic scales of IGW model, determining RO signal fluctuations are the Fresnel scale $\rho_F$ and the outer scale. For radio waves with $\lambda=20$ cm at a GPS–LEO path, $\rho_F$ equals about 1 km, while the vertical outer scale $L_W$ is several $\mathrm{km}$. For inhomogeneities with scales $\geq 1$ km, the anisotropy $\eta$ significantly exceeds its critical value $\eta_{cr}=\sqrt{R_e/H_0}\approx 30$, where $R_e$ is the Earth's radius, and $H_0=6$–$8$ km is the atmospheric scale height. Due to sphericity, different orientations of anisotropic layered inhomogeneities with respect the line of sight result in the saturation of eikonal, or phase fluctuations at $\eta\approx\eta_{cr}$. For a larger anisotropy $\eta\gg\eta_{cr}$, their dependence on $\eta$ degrades, and they remain at the value corresponding to the asymptotic case of spherically-layered inhomogeneities (Gurvich, 1984; Gurvich and Brekhovskikh, 2001). Therefore, for RO sounding, the approximation of strongly anisotropic IGW inhomogeneities $\eta=\mathrm{const}\gg\eta_{\mathrm{cr}}$ is acceptable. The structure characteristic for dry air $C^2_{W,dry}$ is expressed in terms of the conventional parameters determining the 1D vertical spectrum of temperature fluctuations in the IGW model, $V_{\delta T/T}\left(\kappa_z\right)=\beta\frac{\omega^4_{B.V.}}{g^2}\kappa_z^{-3}$ (Smith et al., 1987; Fritts, 1989; Tsuda et al., 1991), as follows (Sofieva et al., 2009):

$$C^2_{W,dry}=\frac{3\beta\omega^4_{B.V.}}{4\pi g^2} \tag{3}$$

where $\beta\approx$0.1 is the coefficient introduced in the IGW model, $\omega_{B.V.}$ is the Brunt–Väisälä frequency, and $g$ is the gravity acceleration.

To obtain the value of the structure characteristic $C^2_W$ in the radio band, $C^2_{W,dry}$ must be multiplied with the coefficient $K^2$, which equals the ratio of the square of the difference of actual and adiabatic vertical gradients of the full refractivity, include the humidity term, and the corresponding value for the dry refractivity (Tatarskii, 1971; Good et al., 1982; Tsuda et al., 2000). The inner scale $l_W$ may vary in the stratosphere from several meters to sever tens of meters (Gurvich and Kan, 2003b; Sofieva et al., 2007a). For locally homogeneous random fields, the power exponent of purely power-law spectra must lie in the following limits: $3 < \mu < 5$ (Rytov et al., 1989a, b). This dictates the necessity of introduction of the outer scale, although the variance of amplitude fluctuations only indicates a weak dependence from the outer scales up to $\mu$ <6 (Gurvich and Brekhovskikh, 2001).

For $\mu = 11/3$, $\eta = 1$, $A = 0{,}033$, and $C_K^2 = C_n^2/\bar{N}^2$, where $C_n^2$ is the structure characteristic of refractivity fluctuations, spectrum (2) $\Phi = \Phi_K$ is a model of the Kolmogorov isotropic turbulence (Monin and Yaglom, 1975). In a stably stratified atmosphere, turbulence is developed mostly in separate layers with vertical scales from several tens of meters to one kilometer. We use the characteristic scale of these layers as the estimate of the outer scale of isotropic turbulence. The inner scale in the spectrum of the Kolmogorov turbulence can be defined as $l_K \approx 6.5\lambda_K = 6.5\nu_a^{3/4}\varepsilon_k^{-1/4}$, where $\lambda_K$ is the Kolmogorov scale, $\nu_a$ is the kinematic molecular viscosity, $\varepsilon_k$ is the kinetic energy dissipation rate (Tatarskii, 1971).

### 2.2 Approximations of Phase Screen and Weak Fluctuations

Due to the exponential decay of air density with the altitude, a ray propagating in the atmosphere is mainly affected by the vicinity of the ray perigee, with the effective size along the ray of about several hundreds of kilometers. The distance from the perigee to the LEO is much greater, and equals about 3000 $\mathrm{km}$. This allows the approximation of the atmosphere as thin screen that only introduces phase variations, including both regular and random ones. The amplitude fluctuations are formed due to the diffraction during the propagation in the free space from the screen to the receiver. We position the phase screen in the plane crossing the Earth's center and perpendicular to the incident rays. The properties of the equivalent phase for RO observation geometry have been studied, for example, in (Hubbard et al.; Gurvich, 1984; Gurvich and Brekhovskikh, 2001). The use of the phase screen allows a significant simplification of the RO signal fluctuation analysis, and makes it possible to take into account the regular variation of refraction with the altitude. In the evaluation of the equivalent phase shift (eikonal), it is necessary take into account the Earth's sphericity.

The amplitude fluctuations are considered weak, if their variance is less than unity (Tatarskii, 1971; Ishimaru, 1978). The weak fluctuation approximation makes it possible to derive simple linear relationships linking the 3D spectrum of the atmospheric refractivity fluctuations with the 2D spectrum of amplitude and phase fluctuations of RO signal (Rytov et al., 1989a, b; Gurvich and Brekhovskikh, 2001; Sofieva et al., 2007a). In the optical range, fluctuations are weak for ray perigee altitudes above 25–30 $\mathrm{km}$ (Gurvich and Kan, 2003a, b; Sofieva et al., 2007b). For GPS radio signals, amplitude fluctuations are significantly weaker, because the Fresnel scale is about thousand times greater than that in the optical range. At low altitudes, refractive attenuation also reduces amplitude fluctuations. Below, we will show that the weak fluctuation condition for GPS RO observations can be fulfilled down to an altitude of several kilometers. In the lower troposphere, especially in tropics, the influence of humidity is strong, and amplitude fluctuations may become strong due to multipath propagation. Complicated non-linear relationships for strong fluctuations may significantly aggravate the data analysis. Some of options of the retrieval of inhomogeneity parameters under strong fluctuation conditions are discussed, for example, by Gurvich et al. (2006).

A high velocity of the ray immersion in satellite observations allows using the hypothesis of "frozen" inhomogeneities for mapping measured temporal spectra of signal fluctuations into spatial spectra.

Atmos. Meas. Tech. Discuss., https://doi.org/10.5194/amt-2017-190
Manuscript under review for journal Atmos. Meas. Tech.
Discussion started: 27 July 2017


## 3 Relationships for Statistical Moment of RO Signal Parameters

The approximations of phase screen and weak fluctuations allow deriving simple expressions for the statistical moments of RO signal fluctuations. In this Section, we will discuss the relationships that link the measured variances and 1D spectra of RO signal fluctuations with 3D spectra of atmospheric refractivity fluctuations for IGW and turbulence models, as well as the model profiles of variances of RO signal fluctuations.

### 3.1 Correlation Functions and Spectra

For a satellite-to-satellite path, using the approximations of phase screen and weak fluctuation, it is possible to derive the following 2D correlation functions in the observation plane $(z_0, y_0)$ (Rytov et al., 1989b):

$$B_{\chi,S}(\Delta z_0, \Delta y_0) = $$
$$= \frac{1}{2}\left\{\tilde{B}_S(\Delta z, \Delta y) \mp \frac{k\gamma}{4\pi x_1 q^{1/2}} \iint \tilde{B}_S(\Delta z', \Delta y') \sin\left[\frac{k\gamma}{4x_1 q}(\Delta z' - \Delta z)^2 + \frac{k\gamma}{4x_1}(\Delta y' - \Delta y)^2\right] d\Delta z' d\Delta y'\right\}$$
$$B_{\chi S}(\Delta z_0, \Delta y_0) = $$
$$= \frac{1}{2}\frac{k\gamma}{4\pi x_1 q^{1/2}} \iint \tilde{B}_S(\Delta z', \Delta y') \cos\left[\frac{k\gamma}{4x_1 q}(\Delta z' - \Delta z)^2 + \frac{k\gamma}{4x_1}(\Delta y' - \Delta y)^2\right] d\Delta z' d\Delta y' \quad (4)$$

where $\chi$ is the logarithmic amplitude, $S$ is the phase, $k = 2\pi/\lambda$, axis $x_0$ is collinear with the incident ray direction, axis $z_0$ is vertical,$\gamma = \frac{x_t + x_1}{x_t}$, $x_t$ is the distance from the transmitter to the phase screen, $x_1$ is the distance from the phase screen to the receiver, $q$ is refractive attenuation coefficient, $\Delta z, \Delta y$ are the scales in the phase screen, defined as the coordinate differences of the phase stationary points, and linked to the corresponding scales in the observation plane by the following relationships: $\Delta z = \frac{q}{\gamma}\Delta z_0, \Delta y = \frac{1}{\gamma}\Delta y_0$, $\tilde{B}_S(\Delta z, \Delta y)$ is the correlation function of the phase in the phase screen, $B_{\chi S}$ is the mutual correlation function of the logarithmic amplitude and phase. The negative sign in the upper formula in (4) applies to the amplitude, and the positive sign applies to the phase.

Taking the Fourier transform, we arrive at the following expressions for the 2D fluctuation spectra of the received signal:

$$F_{\chi,S}(\kappa_z, \kappa_y) = \frac{k^2}{2}\left\{1 \mp \cos\left[\frac{x_1 q}{k\gamma}\left(\kappa_z^2 + q^{-1}\kappa_y^2\right)\right]\tilde{F}_\varphi(\kappa_z, \kappa_y)\right\}$$
$$F_{\chi S}(\kappa_z, \kappa_y) = \frac{k^2}{2}\sin\left[\frac{x_1 q}{k\gamma}\left(\kappa_z^2 + q^{-1}\kappa_y^2\right)\right]\tilde{F}_\varphi(\kappa_z, \kappa_y) \quad (5)$$

where $\tilde{F}_\varphi(\kappa_z, \kappa_y)$ is the 2D spectrum of the fluctuation of eikonal $\varphi = S/k$ in the phase screen. For the sake of convenience, relationships (5) are written in terms of wavenumbers $\kappa_z, \kappa_y$ in the phase screen, which are linked to the wavenumber in the observation plane by the inverse scale relations.

In the general case, the relationship between the 2D spectrum of the eikonal fluctuations in the phase screen $\tilde{F}_\varphi$ and 3D spectrum of the atmospheric refractivity fluctuations $\Phi$ for a random field $\nu$ that is locally homogeneous in a spherical layer can be written down as follows (Gurvich, 1984; Gurvich and Brekhovskikh, 2001):

$$\tilde{F}_\varphi(\kappa_z, \kappa_y) = \bar{\Psi}^2 \int \Phi\left(\kappa_z, \sqrt{\kappa_x^2 + \kappa_y^2}\right) \exp\left(-\frac{R_e H_0}{1 + \kappa_z^2 H_0^2}\kappa_x^2\right) \frac{d\kappa_x}{\sqrt{1 + \kappa_z^2 H_0^2}} \quad (6)$$

Atmos. Meas. Tech. Discuss., https://doi.org/10.5194/amt-2017-190
Manuscript under review for journal Atmos. Meas. Tech.
Discussion started: 27 July 2017


where $\bar{\Psi}$ is the mean eikonal. In particular, for the exponential atmosphere $\bar{\Psi} = \sqrt{2\pi R_e H_0}\bar{N}$. Formula (6) takes into account the sphericity of the atmosphere, which is essential, if $\eta \geq \eta_{cr}$. A general expression (6) for $\tilde{F}_\varphi$ is derived in (Gurvich and Brekhovskikh, 2001). Here, we will discuss important particular cases.

1. Moderate anisotropy $1 \leq \eta \ll \eta_{cr} \approx 30$. In this case the Earth's sphericity is insignificant, and, assuming $R_e H_0 \to \infty$ and performing integration, we arrive at the following known relationship, applicable for random inhomogeneities, locally homogeneous in the Cartesian coordinate system (Tatarskii, 1971; Rytov et al., 1989b), which we denote $\tilde{F}^i_\varphi$:

$$\tilde{F}^i_\varphi(\kappa_z,\kappa_y) \approx \bar{\Psi}^2\sqrt{\frac{\pi}{R_e H_0}}\Phi(\kappa_z,\kappa_y,0) \tag{7}$$

For the isotropic turbulence, we substitute $\Phi = \Phi_K$ with $\mu = 11/3$ and $\eta = 1$.

2. Strongly anisotropic inhomogeneities $\eta \gg \eta_{cr}$. For $\mu$=5, this case corresponds to the model of saturated IGW, for the large-scale part of the spectrum. In this case, we can write the following expression for the eikonal spectrum $\tilde{F}^a_\varphi$:

$$\tilde{F}^a_\varphi(\kappa_z,\kappa_y) \approx \bar{\Psi}^2\sqrt{\frac{\pi}{1+\kappa_z^2 H_0^2}}\frac{\left(K_W^2+\kappa_z^2+\eta^2\kappa_y^2\right)^{1/2}\Gamma\left(\frac{\mu-1}{2}\right)}{\eta\Gamma\left(\frac{\mu}{2}\right)}\Phi_W(\kappa_z,\kappa_y,0) \tag{8}$$

For strongly anisotropic inhomogeneities, function $\tilde{F}^a_\varphi$ has a sharp peak with respect to its argument $\kappa_y$, and it only differs from 0 in a small area near $\kappa_y = 0$; this corresponds to the asymptotic case of spherically symmetric inhomogeneities. This function can thus be approximated as $\tilde{F}^a_\varphi(\kappa_z,\kappa_y) \approx \tilde{V}^a_\varphi(\kappa_z)\delta(\kappa_y)$, where $\tilde{V}^a_\varphi(\kappa_z)$ is the 1D vertical spectrum of the eikonal in the phase screen, and $\tilde{V}^a_\varphi(\kappa_z)$ is evaluated by integrating (8) with respect to horizontal wavenumbers:

$$\tilde{V}^a_\varphi(\kappa_z) = \int \tilde{F}^a_\varphi(\kappa_z,\kappa_y)\,d\kappa_y = \bar{\Psi}^2 C_W^2\sqrt{\frac{\pi}{1+\kappa_z^2 H_0^2}}\frac{\Gamma\left(\frac{\mu-1}{2}\right)}{\eta\Gamma\left(\frac{\mu}{2}\right)}\exp\left(-\frac{\kappa_z^2}{\kappa_W^2}\right)\left(\mathrm{K}_W^2+\kappa_z^2\right)^{-\frac{\mu}{2}+1}\cdot$$
$$\Gamma\left(\frac{1}{2}\right)U\left(\frac{1}{2},-\frac{\mu-4}{2},\frac{\mathrm{K}_W^2+\kappa_z^2}{\kappa_W^2}\right) \tag{9}$$

where $U(\alpha,\beta;t)$ denotes the hypergeometric function.

The variance of the logarithmic amplitude fluctuation is determined by the scales of the order of the Fresnel zone (Tatarskii, 1971). The vertical Fresnel scale $\rho_F = \sqrt{\pi\lambda x_1 q/\gamma}$ for $\lambda = 19.03$ cm varies from 1260 m at a ray height of about 30 km to about 500 m at a ray perigee height of 2 km; therefore, in our case $\rho_F \gg l_W$. The variances of eikonal and refraction angle fluctuations, and the mutual correlation function of amplitude and phase for such steep 3D spectral with $\mu = 5$ are determined by scales of the order of the outer scale $L_W$. Therefore, for the IGW model, the fluctuations of all the RO signal parameters under discussion are determined by inhomogeneities with relatives large vertical scales, significantly exceeding the inner scale: $\kappa_z \ll \kappa_W$. Then, using the expansion of the hypergeometric function for small arguments $t$, it is possible to derive the following expression (Gurvich, 1984):

$$\tilde{V}^a_\varphi(\kappa_z) \approx 2\pi\bar{\Psi}^2 C_W^2\frac{\left(\mathrm{K}_W^2+\kappa_z^2\right)^{-\frac{\mu}{2}+1}}{(\mu-2)\sqrt{1+\kappa_z^2 H_0^2}} \tag{10}$$

In this case, the vertical fluctuation spectra of $\nu$, which corresponds to relative temperature fluctuations $\delta T/\bar{T}$ for dry atmosphere, $V_W^a(\kappa_z)$, and the eikonal fluctuation spectra $\tilde{V}^a_\varphi(\kappa_z)/\bar{\Psi}^2$ in the phase screen are linked by the following relationship

(Gurvich, 1984):

$$V_W^a(\kappa_z) = 4\pi C_W^2 \frac{\left(\mathrm{K}_W^2 + \kappa_z^2\right)^{-\frac{\mu}{2}+1}}{(\mu - 2)} = \sqrt{1 + \kappa_z^2 H_0^2} \frac{\tilde{V}_\varphi^a(\kappa_z)}{\bar{\Psi}^2} \tag{11}$$

Relationship (11) is written for single-sided spectra for $\kappa_z \geq 0$.

In the observations, we obtain a 1D realization of the signal along the receiver trajectory. During a RO event, the changes of the satellite positions are small with respect to their distance from the phase screen. Moreover, the fluctuation correlation scale along the ray significantly exceeds the correlation scale in the transverse direction (Tatarskii, 1971). Therefore, a measured realization corresponds to the ray displacement in the phase screen by distance $s$ along the projection of the satellite trajectory arc. In the phase screen model, we have to take into account the refractive deceleration of ray immersion, and the vertical compaction of the scales. The observation geometry will be determined by the inclination angle $\alpha$ of the occultation plane, defined as the angle between the immersion direction of the ray perigee and the local vertical in the phase screen. 1D spectra of amplitude and phase fluctuation measured along arc $s$ at angle $\alpha$ can be expressed as follows (Gurvich and Brekhovskikh, 2001):

$$V_{\chi,S}(\kappa_s) = \int F_{\chi,S}(\kappa_s \sin\alpha + \kappa' \cos\alpha, \kappa_s \cos\alpha - \kappa' \sin\alpha)\, d\kappa' \tag{12}$$

Angle $\alpha = 0°$ corresponds to a vertical occultation, and $\alpha = 90°$ corresponds to a horizontal, or tangential occultation. The frequency of amplitude fluctuations $f$ is linked to the wavenumber $\kappa_s$ by the following relationship:

$$\kappa_s = 2\pi f / v_s \tag{13}$$

where $v_s$ is the velocity of the ray perigee projection to the phase screen.

For isotropic inhomogeneities, the characteristic frequencies are determined by the corresponding scales and oblique velocity $v_s$ in the direction at angle $\alpha$. Strongly anisotropic inhomogeneities are intersected by the line of sight, effectively, in the vertical direction, because the effect of the horizontal velocity component is much smaller. The condition of such effectively vertical occultations is as follows (Kan, 2004): $\tan\alpha < \eta$. For $\eta \geq 50$, this condition is fulfilled up to angles $\alpha \approx 89°$, which applies, eventually, to any occultation. For strongly anisotropic inhomogeneities, the 1D vertical spectra of amplitude and phase fluctuations at the receiver, are descirbed by the following simple relationships:

$$V_{\chi,S}^a(\kappa_z) = \frac{k^2}{2}\left[1 \mp \cos\left(\frac{x_1 q}{k\gamma}\kappa_z^2\right)\right] \tilde{V}_\varphi^a(\kappa_z) \tag{14}$$

where $\tilde{V}_\varphi^a(\kappa_z)$ is determined by (10). As above, the negative sign applies to the amplitude, and the positive sign applies to the phase.

### 3.2 Variance of Logarithmic Amplitude Fluctuations

For the fluctuations of logarithmic amplitude, in both models of the 3D spectrum of inhomogeneities, the principle scale is the Fresnel scale $\rho_F$, which significantly exceeds the inner scale. In addition, assuming that the outer scale is much greater than $\rho_F$, we can omit the outer and inner scale in the Eq. (2) for the 3D spectrum and use it as a pure power law.

In the case of strongly anisotropic inhomogeneities $\eta \gg \eta_{cr}$, using (1), (14), and condition $\kappa_z H_0 \gg 1$, we can derive the following expression for the variance of logarithmic amplitude (Gurvich, 1984):

$$\sigma_\chi^2(\eta \gg \eta_{cr}) \approx \frac{k^2}{2}\left\{1-\cos\left[\frac{x_1 q}{k\gamma}\left(\kappa_z^2+q^{-1}\kappa_y^2\right)\right]\tilde{V}_\varphi^a(\kappa_z)\,\delta(\kappa_y)\,d\kappa_y d\kappa_z\right\} = \\ = \frac{\pi^2 C_W^2 \bar{\Psi}^2 k^2}{2H_0(\mu-2)\,\Gamma\left(\frac{\mu}{2}\right)\sin\left(\pi\frac{\mu-2}{4}\right)}\left(\frac{q z_1}{\gamma k}\right)^{\frac{\mu}{2}-1} \quad (15)$$

which, for $\mu = 5$, correspond to the model of saturated IGWs.

For a moderate anisotropy $1 \leq \eta \ll \eta_{cr}$, the corresponding expression can also be found in (Gurvich, 1984):

$$\sigma_\chi^2(\eta \ll \eta_{cr}) = \frac{k^2}{2}\left\{1-\cos\left[\frac{x_1 q}{k\gamma}\left(\kappa_z^2+q^{-1}\kappa_y^2\right)\right]\tilde{F}_\varphi^i(\kappa_y,\kappa_z)\,d\kappa_y d\kappa_z\right\} = \\ = \frac{A\pi^2\sqrt{\pi}C^2\bar{\Psi}^2 k^2\eta}{4\sqrt{R_e H_0}\,\Gamma\left(\frac{\mu}{2}\right)\sin\left(\pi\frac{\mu-2}{4}\right)}\left(\frac{q z_1}{\gamma k}\right)^{\frac{\mu}{2}-1} \quad (16)$$

For $C^2 = C_K^2$, $\mu = 11/3$, $A = 0,033$, and $\eta = 1$, Eq. (16) corresponds to a locally homogeneous turbulence.

In order to analyze the influence of anisotropy upon amplitude fluctuations, consider the ratio of (15) and (16) with the same power exponent $\mu$:

$$\frac{\sigma_\chi^2(\eta \gg \eta_{cr})}{\sigma_\chi^2(\eta \ll \eta_{cr})} = \frac{2}{\sqrt{\pi}(\mu-2)}\frac{\eta_{cr}}{\eta} \quad (17)$$

For $\eta = 1$ and $\mu = 5$, this ratio equals 12, and for $\mu = 11/3$, it equals 20. Therefore, the variance of logarithmic amplitude fluctuations increases with increasing anisotropy $\eta$ for $\eta < \eta_{cr}$, and saturates for $\eta \approx \eta_{cr}$, and for the extreme case of spherically layered inhomogeneities $\eta \approx 100 \gg \eta_{cr}$, the ratio in question is about 10–20. This is a consequence of the geometry of occultations: rays are oriented lengthwise with respect to prolonged inhomogeneities.

### 3.3 Variance of Phase (Eikonal) Fluctuations

The main contribution into phase fluctuations comes from inhomogeneities with vertical scales close to the outer scale. Therefore, it is possible to use the geometric optical approximation for formulas (5) and (14). To this end, we expand the cosine for small arguments into series and neglect the inner scale.

For the variance of phase fluctuations for strong anisotropy $\eta \gg \eta_{cr}$ and outer scale $K_W^{-1} \approx H_0/2\pi$, we obtain:

$$\sigma_S^2(\eta \gg \eta_{cr}) \approx \frac{2\pi\sqrt{\pi}k^2 C_W^2\bar{\Psi}^2\Gamma\left(\frac{\mu-2}{2}\right)}{(\mu-2)\,H_0\Gamma\left(\frac{\mu-1}{2}\right)}\mathrm{K}_W^{-\mu+2} \quad (18)$$

For $\mu = 5$, the variance depends on the outer scale as $\mathrm{K}_W^{-3}$.

For a moderate anisotropy $\eta \ll \eta_{cr}$, using (5) and (7), we obtain the following expression:

$$\sigma_S^2(\eta \ll \eta_{cr}) \approx \frac{2\pi\sqrt{\pi}k^2 A C^2\bar{\Psi}^2\eta}{(\mu-2)\sqrt{R_e H_0}}\mathrm{K}_K^{-\mu+2} \quad (19)$$

For $C^2 = C_K^2$, $\mu = 11/3$, $A = 0,033$, and $\eta = 1$, this corresponds to the model of isotropic turbulence. In this case, the variance of phase fluctuations depends on the outer scale as $\mathrm{K}_K^{-5/3}$ (Tatarskii, 1971). The ratio of (18) and (19) for the same $\mu$, in way similar to amplitude fluctuations, is proportional to the ratio of $\eta_{cr}/\eta$.

### 3.4 Variance of Ray Incident Angle Fluctuations

For a strong anisotropy $\eta \gg \eta_{cr}$, the incident ray direction fluctuations are nearly vertical. The vertical fluctuation spectrum of the ray incident angle is equal to that of eikonal, multiplied by $\kappa_z^2$. Then, replacing the cosine in (14) by unity, we arrive at the following expression for the variance of ray incident angle fluctuations:

$$\sigma_\alpha^2\left(\eta \gg \eta_{cr}\right) \approx \frac{4\pi C_W^2 \bar{\Psi}^2}{\left(\mu-2\right)\left(\mu-4\right) H_0} \mathrm{K}_W^{-\mu+4} \tag{20}$$

and for $\mu = 5$, the variance depends on the outer scale as $\mathrm{K}_W^{-1}$.

For the case $\eta = 1$, the variance of incident angle fluctuations is determined by the inner scale of inhomogeneities, unlike the case of a strong anisotropy. Moreover, the term with the cosine in (5) gives a small contribution, as compared to 1 if $\frac{x_1 q \kappa_K^2}{k\gamma} \gg 1$. Using (5) and neglecting the cosine term, we arrive at the following expression for the fluctuations of the full incident angle $\theta$:

$$\sigma_\theta^2\left(\eta = 1\right) \approx \frac{\pi\sqrt{\pi} A C_K^2 \bar{\Psi}^2 \Gamma\left(2-\frac{\mu}{2}\right)}{2\sqrt{R_e H_0}} \kappa_K^{-\mu+4} \tag{21}$$

For the Kolmogorov turbulence, the variance of incident angle fluctuations depends on the inner scale as $\kappa_K^{1/3}$. Introducing the effective thickness of the atmosphere along the ray, which equals $L_{ef} = \sqrt{\pi R_e H_0} \approx 400\ \mathrm{km}$, we see that (21) coincides with the corresponding formula in (Tatarskii, 1971) for an observation distance of $L_{ef}$ in a homogeneously random medium.

### 3.5 Mutual Correlation of Logarithmic Amplitude and Phase

For the case of a strong anisotropy $\eta \gg \eta_{cr}$, the single-point correlation $\langle \chi S \rangle = B_{\chi S}(0)$ is determined by the outer scale of inhomogeneities. Using (5) and (10), and expanding the sine into series, we arrive at the following formula:

$$\langle \chi S\left(\eta \gg \eta_{cr}\right)\rangle = \frac{2\pi C_W^2 \bar{\Psi}^2 k^2}{H_0\left(\mu-2\right)\left(\mu-4\right)} \frac{x_1 q}{k\gamma} \mathrm{K}_W^{-\mu+4} \tag{22}$$

For $\mu = 5$, the correlation depends on the outer scale as $\mathrm{K}_W^{-1}$, which is the same dependence as that of variance of bending angle fluctuations.

For isotropic inhomogeneities, $\eta = 1$, the most important scale determining the correlation of the logarithmic amplitude and phase, is the Fresnel scale $\rho_F \gg l_K$. Under the assumption that $\rho_F$ is small compared to the outer scale, it is sufficient to consider a 3D spectrum $\Phi_K$ in a purely power form. This results in the following formula:

$$\langle \chi S(\eta = 1)\rangle = \frac{\pi^2\sqrt{\pi} A C_K^2 \bar{\Psi}^2 k^2}{4\sqrt{R_e H_0}\Gamma\left(\frac{\mu}{2}\right)\cos\left(\pi\frac{\mu-2}{4}\right)} \left(\frac{x_1 q}{k\gamma}\right)^{\frac{\mu}{2}-1} = \sigma_\chi^2\left(\eta = 1\right)\tan\left(\pi\frac{\mu-2}{4}\right) \tag{23}$$

For $\mu = 11/3$, the relation between correlation $\langle \chi S(\eta = 1)\rangle$ and the variance of amplitude fluctuations is the same as for a homogeneously random medium (Tatarskii, 1971).

### 3.6 Model Variance Profiles

The profiles were evaluated for a GPS–LEO system with orbit altitudes of 20000 km and 800 km, respectively, for a wavelength of 19.03 cm. The parameters of the regular atmosphere, including refractive index $\bar{N}$, the height scale of a homogeneous atmosphere $H_0$, the average eikonal $\bar{\Psi}$, bending angle $\bar{\varepsilon}$, and refractive attenuation coefficient $q$, correspond to the standard model of the atmosphere.

The structure characteristic of the relative fluctuations of refractive index was specified for the model of saturated IGWs in a dry atmosphere, according to relation (3). Numerous radio sound data and observations of stellar occultations indicate that this relation is met with a good accuracy for the troposphere and stratosphere. For the radio band, the structure characteristic was multiplied by $K^2$ in order to take humidity into account. We were using the humidity profile, typical for spring and autumn in middle latitudes, with the gradient scale of 2.5 $\mathrm{km}$. As shown above, the inner scale of the inhomogeneities is insignificant in the IGW model. The outer scale, corresponding to vertical scale of dominant waves, was assumed to equal $L_W = 4\ \mathrm{km}$ (Smith et al., 1987; Tsuda et al., 1991).

For the isotropic turbulence at heights of 4–15 $\mathrm{km}$, we used numerous data of radar measurements of the structure characteristic performed during years 1983–1984 in Platteville, Colorado (Nastrom et al., 1986). From the monthly averaged profiles of $C_n^2$ shown in Fig. 10 of the cited paper, we chose the maximum values that mostly correspond to August, in order to obtain the upper estimate of turbulent fluctuations of RO signals. For heights of 15–30 $\mathrm{km}$, where humidity is negligible, we used model data $C_n^2$ from (Gracheva and Gurvich, 1980), which generalizes the results of numerous observations and models for the dry optical turbulence (Gurvich et al., 1976), as well as retrievals of $C_n^2$ from stellar occultations (Gurvich and Kan, 2003b; Sofieva et al., 2007a). For the outer scale we used the value of 1 $\mathrm{km}$. The inner scale is assumed to increase from 4 $\mathrm{cm}$ at 4 $\mathrm{km}$ to 0.75 $\mathrm{m}$ at 30 $\mathrm{km}$. The mean value of refraction angle $\bar{\varepsilon}$ and refractive attenuation coefficient $q$ were evaluated using the exponentially decaying atmospheric air density profile:

$$\bar{\varepsilon} = -\frac{\bar{\Psi}}{H_0}, \quad q = \left(1 - \frac{x_1}{\gamma}\frac{\bar{\varepsilon}}{H_0}\right)^{-1} \tag{24}$$

Figure 1 shows the model profiles of rms fluctuations of the logarithmic amplitude, eikonal, incident angle, as well as the correlation of the logarithmic amplitude and eikonal, for saturated IGWs and isotropic turbulence. For the assumed parameters of the 3D inhomogeneity spectra, all the rms for saturated IGWs exceed the corresponding values for the isotropic turbulence by an order of magnitude or even more, and this difference increases with the altitude. This especially applies to the eikonal fluctuations and amplitude-eikonal correlation, where the difference in rms exceeds two orders of magnitude. The knee of the profiles at an altitude of 10 $\mathrm{km}$ for the turbulence model is linked to the peculiarity of the measured profiles of $C_n^2$ (Nastrom et al., 1986). In (Nastrom et al., 1986) it is, however, noted that the increase of $C_n^2$ above 10 $\mathrm{km}$ is not corroborated by other observations in Platteville (Ecklund et al., 1979) and can be attribute to measurement noise. For the IGW model, the knee is explained by the abrupt change of the Brunt-Väisälä frequency near the tropopause, according to (3).

For the turbulence model, we assumed the outer scale to be equal to 1 $\mathrm{km}$. However, for stable stratification, which is typical for the stratosphere, the outer scale may be significantly less than this value, down to hundreds or even tens of meters (Wheelon, 2004). The saturation of the 3D spectrum of turbulence at the outer scale, which is less than the Fresnel zone size, will result in the decrease of the turbulent fluctuations of RO signals as compared to the estimates for 1 $\mathrm{km}$, and the difference with IGW fluctuations will be even larger. Due to the fact that the averaging over the Fresnel scale results in much smaller amplitude

Atmos. Meas. Tech. Discuss., https://doi.org/10.5194/amt-2017-190
Manuscript under review for journal Atmos. Meas. Tech.
Discussion started: 27 July 2017


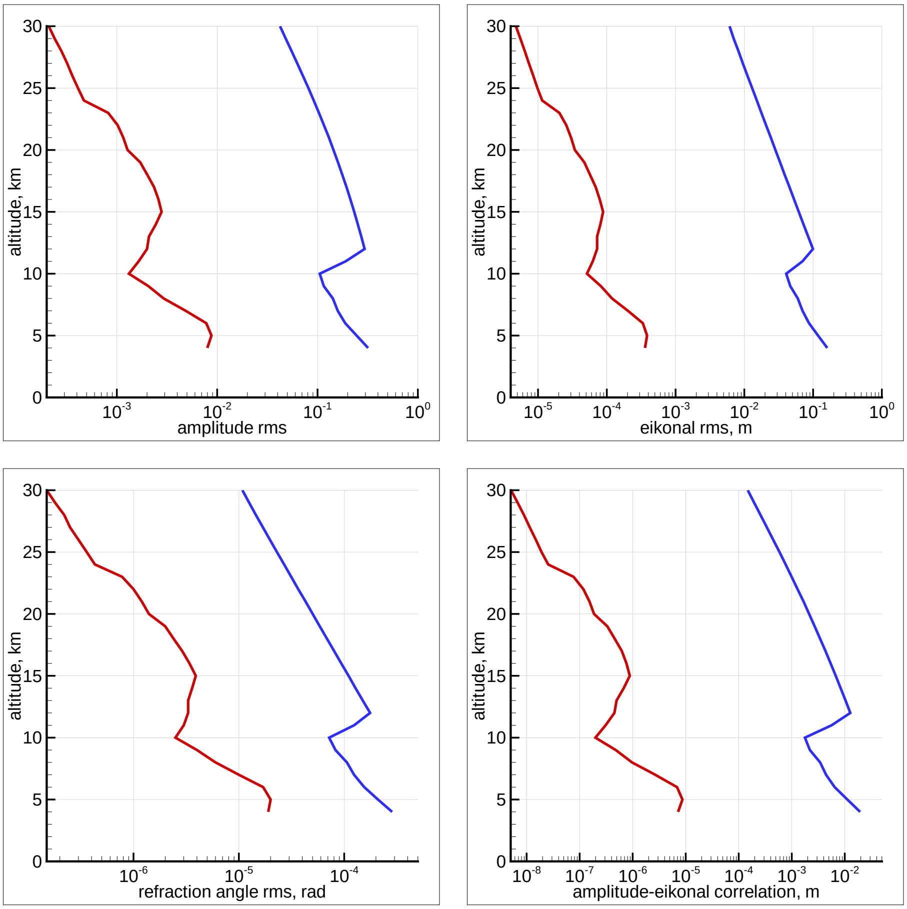


**Figure 1.** RMS fluctuations of logarithmic amplitude, eikonal, incident angle, and single-point correlation of logarithmic amplitude and phase for the model of saturated IGWs (blue lines) and for the model of turbulence (red lines).

fluctuations of RO signal as compared to the optical band, the weak fluctuation condition is fulfilled down to the lower limit of the altitude range under discussion.

A significant variability of the parameters of atmospheric inhomogeneities, especially structure characteristics, depending on latitude, season, orography, intermittence etc., implies that the averages model profiles only allow for rough estimates of RO signal fluctuations. The aim of our work is, however, an approximate estimation of the contributions of fluctuations caused by different inhomogeneity types. Anyway, our estimates of the difference between the contributions of IGWs and turbulence are large enough to ensure that the IGWs play a dominant role under the conditions in question.

Atmos. Meas. Tech. Discuss., https://doi.org/10.5194/amt-2017-190
Manuscript under review for journal Atmos. Meas. Tech.
Discussion started: 27 July 2017


Atmospheric Measurement Techniques
Discussions

## 4 Experimental Fluctuation Spectra of Amplitude and Phase

The most important difference between turbulence and saturated IGWs is the anisotropy of the latter. The variances of RO signal parameter fluctuations, being single-point characteristics, do not contain an immediate information on the anisotropy of the 2D field of RO signal fluctuation in the observation field, to which the anisotropic 3D field of atmospheric inhomogeneities is mapped. This information can be extracted from 1D spectra of RO signal fluctuations, measured at different angles with respect to the local vertical. For turbulence, due to its isotropy, the fluctuation frequencies of the signal are determined by the characteristic scales and the oblique movement velocity $v_s$ of the line of sight. For anisotropic IGW inhomogeneities, they fluctuation frequencies of the signal are determined by the vertical velocity $v_v$ for the majority of occultations. These velocities and frequencies coincide for a vertical occultation, but they may differ several tens of times for strongly oblique occultation, due to the geometrical difference between the vertical and oblique velocity and refractive damping of the vertical velocity. This frequency discrimination of isotropic and anisotropic fluctuations in oblique occultations allows for a separate estimate of their contribution into signal fluctuation spectra (Gurvich and Kan, 2003a, b; Sofieva et al., 2007a, b).

Figures 2 and 3 show the spectra of relative fluctuations of the amplitude for the wavelength $\lambda_1 = 19.03$ cm from GPS/MET observations acquired on February 15, 1997. Figure 2 shows the spectra for the low stratosphere at altitudes from 25 km down to the upper boundary of the tropopause located at 9–13 km. Figure 3 shows the spectra for the upper troposphere at altitudes from 8–12 km down to 4 km. As noted above, the analysis is based on occultation events with different inclination angles, in middle and polar latitudes. We selected events with a low level of ionospheric fluctuations at altitudes below 60–70 km. Under these conditions, below 25–30 km neutral atmospheric signal fluctuations will supersede the ionospheric fluctuations and measurement noise. Noise correction was performed under the assumption that the noise source is the receiver, and the noise properties remain constant during an occultation event. The noise spectrum was estimate from the occultation data records at altitudes of 70–50 km with a low level of neutral atmospheric and ionospheric fluctuations. The mean amplitude profiles were determined from linear trends. Figure 2 and 3 (as well as Figure 4 and 5 below) show 30 examples of stratospheric events and 20 examples of tropospheric events. For the stratosphere, the inclination angles changed within the range of $20° - 87°$, for the troposphere they changed in the range of $35° - 88°$. Therefore, for strongly anisotropic inhomogeneities, these occultations were effectively vertical.

The amplitude fluctuation spectra are represented as the product of wavenumber and spectral density, normalized to the variance. Such a product will be hereinafter referred to as the spectrum, as distinct from the spectral density. The spectra indicate a maximum corresponding to the Fresnel scale. The theoretical spectra for both inhomogeneity types have asymptotics with a slope of $+1$ for low frequencies; for IGWs, the asymptotics corresponds to the condition $L_W \to \infty$. For the high frequencies, at the diffractive decline, the slope of the spectra is $-\mu + 2$, i.e. $-3$ for the IGW model, according to formulas (10) and (14), and $-5/3$ for turbulence (Tatarskii, 1971; Gurvich and Brekhovskikh, 2001; Woo et al., 1980). For the chosen fragments of realizations, we used the Hann cosine window. This window allows the minimization of distortions of spectra with a steep decrease (Bendat and Piersol, 1986). The Fourier periodograms were averaged with a spectra window of a variable width $\Delta f$: first with a window of a constant Q-factor $f/\Delta f = 2$, then with a window of a constant width. The spectra were normalized to

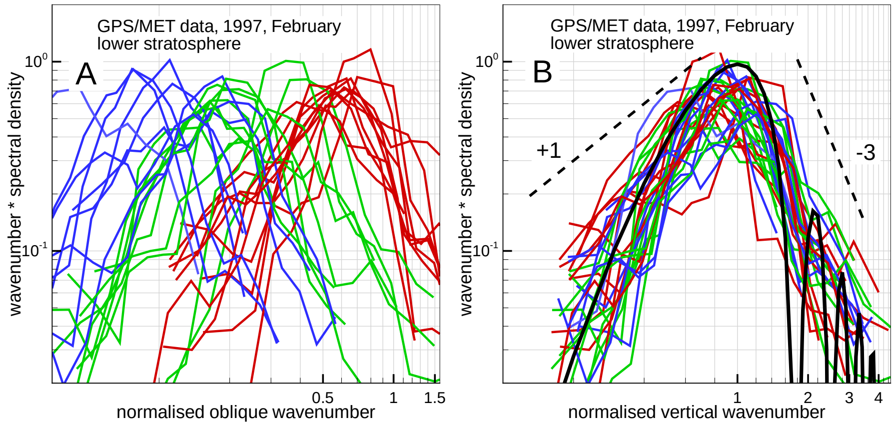


**Figure 2.** Amplitude fluctuation spectra for the lower stratosphere: panel A: the isotropy hypothesis; panel B: the anisotropy hypothesis. The color map red–green–blue corresponds to the increasing occultation angles, which are subdivided into three groups. The black solid line in panel B presents the theoretical vertical spectrum for the saturated IGW model; the dashed lines present the asymptotics of this spectrum for low and high frequencies, the low-frequency asymptotic is evaluated for $L_W \to \infty$.

the variance, evaluated as the integral of the spectral density over frequency. The spectra in Figure 2 and 3 are plotted in two forms. In panels A, they are plotted as functions of the oblique wavenumber, according to the isotropy hypothesis; in panels B, they are plotted as functions of the vertical wavenumber, according to the anisotropy hypothesis for effectively vertical occultations. The ray perigee velocities and occultation angles were evaluated from the satellite orbit data. The wavenumbers were normalized on the Fresnel scale in the corresponding direction, i.e., the values along the horizontal axis are $2\pi\kappa_s\rho_F(\alpha)$ for the isotropy hypothesis and $2\pi\kappa_z\rho_F(\alpha = 0)$ for the anisotropy hypothesis. For this normalization, the spectral maxima must correspond to the argument equal to 1.

Figure 2 and 3 indicate that for the isotropy hypothesis, panels A, the spectral maxima are spread over about 1.5 decade of frequencies. With the increasing occultation angle, the maxima systematically shift to lower frequencies, although, the oblique velocities, on the contrary, increase. In panels B, all the spectra are grouped around the vertical Fresnel scale, which favors the anisotropy hypothesis. For the verification of the isotropy/anisotropy hypotheses, strongly oblique occultations should be most informative. If the amplitude spectra contained a significant isotropic component, it should manifest itself in oblique spectra as an additional maximum at higher frequencies. In stellar scintillation spectra, such a double-hump structure is typical (Gurvich and Kan, 2003a, b; Sofieva et al., 2007a). The absence of the second high-frequency maximum in Figures 2 and 3 indicates that the amplitude fluctuations caused by the isotropic turbulence in these measurements were significantly weaker compared to those caused by the anisotropic inhomogeneities. The experimental amplitude spectra in panels B are in a good agreement with the theoretical spectrum (10) and (14). Although the variance of amplitude fluctuations weakly depends on the outer scale $L_W$, if it significantly exceed the Fresnel scale, still, the influence of $L_W$ is noticeable in the low-frequency spectral region, where it results in a faster than +1 decrease of the spectrum for decreasing frequencies. This effect was utilized for the

Atmos. Meas. Tech. Discuss., https://doi.org/10.5194/amt-2017-190
Manuscript under review for journal Atmos. Meas. Tech.
Discussion started: 27 July 2017


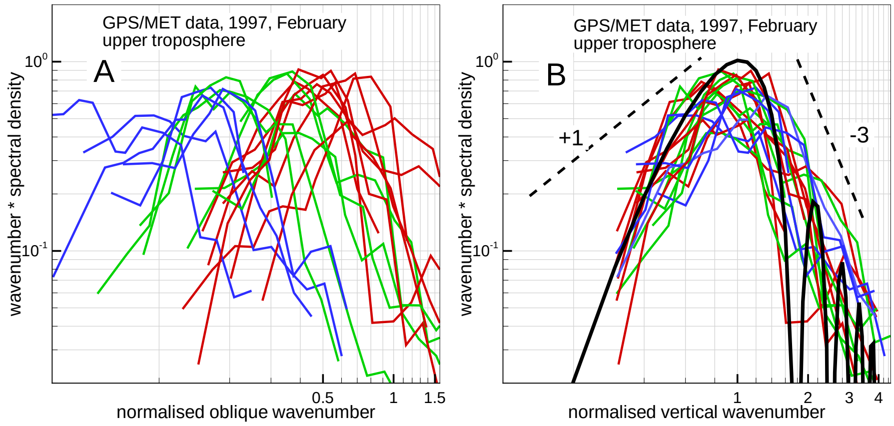


**Figure 3.** Amplitude fluctuation spectra for the upper troposphere: panel A: the isotropy hypothesis; panel B: the anisotropy hypothesis. The notations are the same as in Figure 2

retrieval of internal gravity wave and turbulence parameters from stellar scintillations (Sofieva et al., 2007a). For the theoretical spectrum in the stratosphere, we used the value of $L_W = 2.0$ km; for the troposphere, we used the value of $L_W = 1.2$ km. Deep oscillations of the theoretical spectrum in the high-frequency region are caused by diffraction on a thin screen. The slope of our spectrum at their diffractive decline agrees with the theoretical value $-3$; note, the diffractive slope of the spectral density equals $-4$. The fact that all the spectra in panels B group together means that all the angles $\alpha$ met the condition of effectively vertical occultations. For $\alpha_{\max} = 88°$, we can estimate anisotropy $\eta > \tan(\alpha_{\max}) \approx 30$ for the inhomogeneities, whose vertical scale equals the Fresnel scale.

The measured RMS values of the relative fluctuations of the amplitude in the stratosphere are 0.08–0.20, which is in a fair agreement with the IGW model (Figure 1), which equals 0.17 in the middle of the height range. For the upper troposphere, the measured RMS values are 0.12–0.35 and, therefore, they mostly exceeds the theoretical estimate, which equals 0.16. The experimental RMS values indicate the applicability of the approximation of weak fluctuations for the interpretation of these data.

The phase in RO observations is presented as the excess phase, which equals the difference between the full eikonal and the straight-line satellite-to-satellite distance. We will refer to the excess phase as to the eikonal. Double-frequency observations allow for the exclusion of the ionospheric component of the eikonal under the assumption that the trajectories of the two rays coincide. The ionospheric corrected eikonal consists of two components: 1) the neutral atmospheric eikonal evaluated as the integral along a straight ray, which in Section 3 was denoted as $\Psi$, and 2) the addition to the geometrical length of the ray due to refraction (Vorob’ev and Krasil’nikova, 1984; Gurvich et al., 2000). The second term is approximately equal to the first one at a height of 15 km, and it rapidly increases for lower altitudes. In the first approximation, the eikonal variations are completely determined by the refractive index variations in the first term (Vorob’ev and Krasil’nikova, 1984). Strong regular variations of the eikonal with the altitude, and its relatively small fluctuations, which amount to tenths of percent, aggravate the

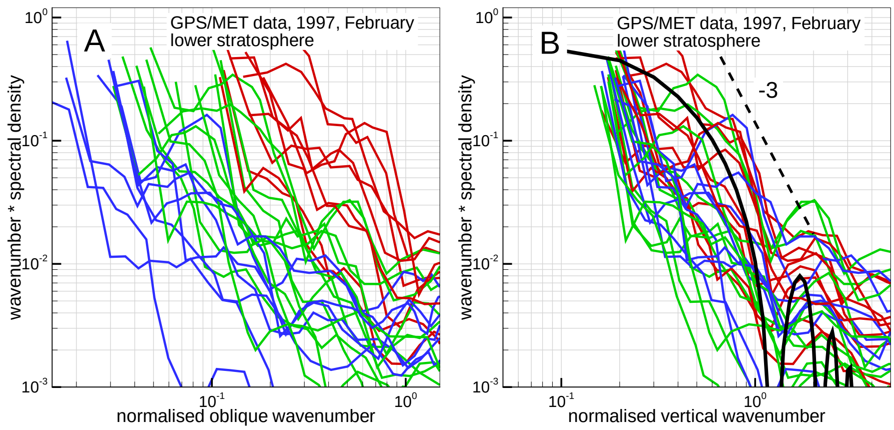


**Figure 4.** The normalized eikonal fluctuation spectra for the lower stratosphere: panel A: the isotropy hypothesis; panel B: the anisotropy hypothesis. The black solid line in panel B represents the theoretical vertical spectrum for the saturated IGW model; the dashed line represents its asymptotics. Cf. the caption of Figure 2.

separation of fluctuations, especially due to the difficulty of the evaluation of the mean eikonal profile (Gurvich et al., 2000; Cornman et al., 2012; Tsuda et al., 2000). In this study, we use the smooth eikonal profile evaluated for the MSISE-90 model (Hedin, 1991) complemented with a simple model of humidity: the relative humidity has a constant value of 80% below 15 $\mathrm{km}$. These profiles are evaluated for the real observation geometry and they correctly represent both the atmospheric eikonal and the geometrical length of the ray. Still, both before and after the subtraction of the model profiles, the eikonal realizations contained low-frequency trends, due the model inaccuracy. We applied an additional detrending square-polynomial term to the eikonal deviation from the model. This procedure smooths the spectral components with scales exceeding the half-length of the realization. Similar to the amplitude spectra, we used the Hann window also for the eikonal.

Figure 4 and 5 present the normalized spectra of the atmospheric fluctuations of the eikonal for the same events and altitude ranges as for the amplitude spectra. The eikonal fluctuation spectra are also represented as the product of wavenumber and spectral density. In this representation, the slope of the theoretical eikonal spectra equals $-\mu+2$ and, correspondingly, it equals $-3$ for IGWs and $-5/3$ for turbulence. The eikonal spectra normalized according to the anisotropy hypothesis have a somewhat large spread compared to the amplitude spectra, still, they also corroborate the dominant role of anisotropic inhomogeneities. These spectra are in a fair agreement with the theoretical vertical spectrum (14). For the evaluation of the theoretical spectrum, we used the same value of the outer scale as for the amplitude spectra.

For the stratosphere, the measured RMS values of the eikonal fluctuations are 3–10 $\mathrm{cm}$, while their estimate was 5 $\mathrm{cm}$. For the upper troposphere, the measured RMS were 4–15 $\mathrm{cm}$, while their theoretical was about 7 $\mathrm{cm}$.

Atmos. Meas. Tech. Discuss., https://doi.org/10.5194/amt-2017-190
Manuscript under review for journal Atmos. Meas. Tech.
Discussion started: 27 July 2017


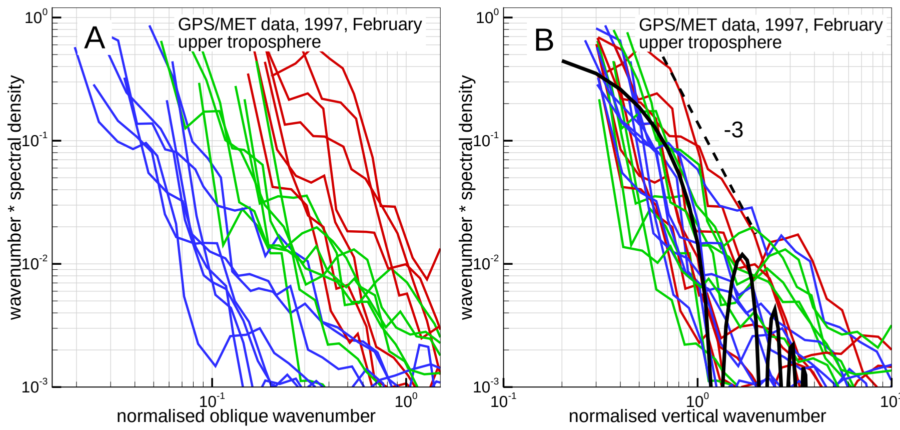


**Figure 5.** The normalized eikonal fluctuation spectra for the upper troposphere. Panel A: the isotropy hypothesis; panel B: the anisotropy hypothesis. The notations are the same as in Figure 4.

## 5 Discussion

In this study, we discussed the 3D spectra of atmospheric inhomogeneities of two types: 1) the isotropic Kolmogorov turbulence, and 2) the anisotropic saturated IGWs. For RO observations, in the approximations of the phase screen and weak fluctuations, we derived the relationships that link the observed 1D fluctuation spectra of the amplitude and phase with the 3D inhomogeneity spectra. This allowed us to obtain the analytical expressions for the variances of the amplitude, phase, and ray incident angle fluctuations, as well as the single-point amplitude-phase correlation for both inhomogeneity types. The theoretical estimates of the variances of RO amplitude and phase fluctuations for different values of the parameters of atmospheric inhomogeneity model, including the structure characteristics and vertical scales, for middle latitudes in the stratosphere and upper troposphere, indicate that the major contribution into RO signal fluctuations comes from saturated IGWs. The contribution of the Kolmogorov turbulence, under these conditions, is small. Even taking into account a significant spread of possible values of the structure characteristics and typical scales of inhomogeneities, it is hard to expect that this can compensate the difference between the IGS and turbulence in this altitude range. Moreover, the averaging of RO signal fluctuations along the whole ray inside the atmosphere damps the influence of intermittence, which is typical for turbulence under stable stratification conditions.

From GPS/MET data acquired on February 15, 1997, we evaluated the variances and spectra of the relative fluctuations of amplitude and the fluctuations of phase for the lower stratosphere, comprising the altitudes from 25 $\mathrm{km}$ down to the upper boundary of the tropopause, and for the upper troposphere, comprising the altitudes from the upper boundary of the tropopause down to 4 $\mathrm{km}$. For analysis, we chose RO events in middle and polar latitudes with different occultation trajectories: from vertical ones with occultation angle near 0 degree to strongly oblique ones with occultation angles up to 88 degree. The experimental spectra of the amplitude and phase fluctuations, presented as a function of vertical wave numbers for the anisotropy hypothesis or oblique wavenumbers for the isotropy hypothesis, indicate a strong anisotropy of the atmospheric inhomogeneities. This, along with the theoretical estimates signifies the dominant role of saturated IGWs for RO signal fluctuations. The experimental estimates of variances of amplitude and phase fluctuations mostly agree with evaluations based on the IGW model.

In comparison with the optical band, the radio band is characterized by a much greater Fresnel scale $\rho_F$. This, together with the strong refractive attenuation, significantly reduces the amplitude fluctuations at small altitudes, and, therefore, the weak fluctuation condition is met for altitudes down to a few kilometers. This is corroborated by the measured variance of relative amplitude fluctuation. The upper boundary of the RO monitoring of atmospheric inhomogeneities is close to the lower boundary of optical occultations. Therefore, radio and optical occultations, together with the simple approximations, give an opportunity of monitoring the wave activity over the whole stratosphere and upper troposphere.

Satellite observations of stellar occultations indicate that in the optical band, at the perigee height about 30 $\mathrm{km}$, IGWs and the Kolmogorov turbulence give comparable contributions into the variance of intensity fluctuations (Gurvich and Kan, 2003a, b; Sofieva et al., 2007a, b). In the radio band, due to the larger Fresnel scale, the role of large-scale inhomogeneities with a steeper 3D spectrum increases. Such inhomogeneities are attributed to IGWs (Kan et al., 2002). This follows from (15) and (16): the decay of variance with increasing wavelength $\sigma_\chi^2 \propto \lambda^{\mu/2-3}$, is stronger for turbulence, $\lambda^{-7/6}$, than for IGWs, $\lambda^{-1/2}$. The relative contribution of IGWs into the variance of amplitude fluctuations with respect to that of isotropic turbulence in the radio band, compared to the optics, increases proportionally to $(\lambda_{GPS}/\lambda_{opt})^{2/3} \approx 5 \cdot 10^3$. This difference is also seen in Figure 1, which shows the amplitude RMS at an altitude of 30 $\mathrm{km}$, if we recollect that in the optical band, the amplitude fluctuations due to IGWs are additional restrained by the inner scale of IGWs that exceeds the Fresnel scale by about an order of magnitude.

The statistical analysis of eikonal fluctuations is aggravated by the fact they are non-stationary, and one of the main problem is the determination of the mean profile. We evaluated the eikonal spectrum using two different mean profiles: 1) the model profile and 2) the profile obtained by the sliding averaging of the eikonal profile over an altitude windows with a half width of $\Delta h$, with the subsequent detrending the eikonal fluctuations. The use of mean eikonal obtained the sliding averaging with $\Delta h$=5 $\mathrm{km} > L_W$ and the model profile resulted in very close spectra. A disadvantage of the sliding averaging consists in the fact that it requires additional interval $\Delta h$ in the beginning and in the end of a realization.

For strongly anisotropic inhomogeneities, RO signal fluctuations are determined primarily by the vertical structure of inhomogeneities and, accordingly, by the vertical velocity of the ray immersion for different occultation angles $\alpha$. The comparison of amplitude records taken as a function of time or as a function of perigee height clearly indicates that for different $\alpha$, the temporal dependencies have different characteristic frequencies, while the altitudinal dependencies have close periods. In the tropics, in the lower troposphere, below the altitude of 7 $\mathrm{km}$, the type of the vertical dependence of the amplitude abruptly changes: the fluctuation frequencies increase, and their magnitude significantly exceeds that at the same altitudes in middle and polar latitudes (Sokolovskiy, 2001, e.g.). In order to obtain a qualitative estimate of the humidity influence, we additionally analyzed the amplitude spectra in the upper and lower troposphere from the COSMIC data in tropics, May 2011, and in middle and polar latitudes, January 2011. For each latitude band, we chose 30 occultations, with occultation angles varying from $45°$ to $89°$. In the tropics and upper troposphere, at altitudes from 13 down to 8 $\mathrm{km}$, in the amplitude spectra the dominant role is played by anisotropic IGWs. In the lower troposphere, at altitudes from 6 down 1 $\mathrm{km}$, however, the spectra mostly agree with

Atmos. Meas. Tech. Discuss., https://doi.org/10.5194/amt-2017-190
Manuscript under review for journal Atmos. Meas. Tech.
Discussion started: 27 July 2017


the Kolmogorov turbulence, although some of the spectra have maxima located at higher frequencies, as compared to what is predicted by the theory. This may be a consequence of strong fluctuations, because the relative amplitude fluctuation RMS in tropics, in this altitude range is close to unity. A similar analysis for altitudes from 6 to 1 $\mathrm{km}$, for middle and polar latitudes in January, where the humidity influence was much smaller, indicates that the amplitude spectra mostly correspond to the IGW model, and the fluctuation RMS was smaller than in the tropics, and was equal to 0.2–0.6. This indicates that in the framework of the approximations of the thin screen and weak fluctuations, for the lower troposphere, it is only possible to infer rough estimates. A strict quantitative analysis would require more advanced techniques.

The main result of this study consists in the statement that in the stratosphere and upper troposphere, at altitudes above 4-5 $\mathrm{km}$ for middle and polar latitudes, and above 7-8 $\mathrm{km}$ in the tropics, the dominant contribution into RO signal fluctuations comes from anisotropic inhomogeneities described by the saturated IGW model. Formerly, for the stratosphere, in the altitude range 15–30 $\mathrm{km}$, this was demonstrated by Steiner et al. (2001), who showed that the temperature fluctuation spectra obtained from GPS/MET observations, in the vertical scale range 2–5 $\mathrm{km}$ are in a satisfactory agreement with the saturated IGW model. Wang and Alexander (2010) and McDonald (2012), analyzing collocated temperature profiles from COSMIC observations, showed that in the stratosphere, the most large-scale dominant temperature perturbations are of wave nature. Gubenko et al. (2008, 2011) developed a method for the determination of the basic characteristics of dominant IGWs, including their intrinsic frequency and phase velocities from vertical profiles of temperature. The method was validated on high-resolution radiosonde observations of temperature and wind and then applied to the analysis of IGW based on temperature profiles retrieved from RO observations in COSMIC and CHAMP missions.

On the other hand, Steiner et al. (2001) only analyzed filtered temperature profiles with scales exceeding 1.5–2 $\mathrm{km}$. The RO signal spectra, as shown in Figures 2–5, have a significantly higher resolution, and the main limitation is imposed by noise. The principle parameters of IGWs are their structure characteristic $C_W^2$ and outer scale $\mathrm{K}_W^{-1}$. Our estimates indicate that humidity fluctuations in middle and polar latitudes are significant below altitudes of 5–6 $\mathrm{km}$; for high altitudes, temperature fluctuations dominate. The relation between $C_{W,dry}^2$ with the traditional IGW parameters is given by (3). The outer scale is introduced in our model in such way that the inhomogeneity spectrum is saturated to a constant for $\kappa_z < \mathrm{K}_W$ (Smith et al., 1987). The temperature variance in the IGW model can be inferred from (11) (Sofieva et al., 2009):

$$\sigma_{\delta T/T}^2 = \frac{4\pi}{3} C_{W,dry}^2 \mathrm{K}_W^{-2} \tag{25}$$

which, in turn, determines the specific potential energy of waves:

$$E_p = \frac{1}{2}\left(\frac{g}{\omega_{B.V.}}\right)^2 \sigma_{\delta T/T}^2 \tag{26}$$

Tsuda et al. (2000); de la Torre et al. (2006); Khaykin et al. (2015) (further references can be found in these papers) studied the global morphology of $E_p$ in the stratosphere using $\sigma_{\delta T/T}^2$ evaluated from temperature profiles retrieved from GPS/MET data. The wave activity can be monitored directly from measurements of amplitude and phase fluctuations of RO signals, using the simple relationships that link them to IGW parameters. A simultaneous determination of structure characteristic and outer scale from RO signal fluctuations allow a more detailed study of IGWs. Adjusting the method of the IGW parameter retrieval from stellar occultations (Gurvich and Kan, 2003a; Sofieva et al., 2007a, 2009), it is possible to derive the structure characteristic and outer scale from amplitude spectra. These parameters can also be inferred from eikonal spectra. Still, it is preferable to use amplitude spectra, which are much more sensitive to refractivity fluctuations: phase variations are proportional to refractivity variations, while amplitude variations are proportional to their second derivative (Rytov et al., 1989b). In addition, strong regular variations of the eikonal with the altitude may introduce significant uncertainties in the lower-frequency region of the eikonal spectrum. On the other hand, for express estimates, it possible to use variances only. The amplitude variance allows the determination of the structure characteristic (15); the eikonal variance, together with the estimate of the structure characteristic allow the estimate of the outer scale (18). The maximum frequency of amplitude spectra may indicate what inhomogeneity type is essential for the RO signal fluctuations.

## 6 Conclusions

In this study, we presented simple relationships and theoretical estimates of the amplitude and phase variances of RO signal for typical parameters of 3D spectra based on two models: 1) the Kolmogorov turbulence and 2) saturated IGWs. For GPS/MET observation in the altitude range of 4–25 km for middle and polar latitudes, we derived the amplitude and phase fluctuation spectra. Both theoretical and experimental results indicate a dominant role of saturated IGWs in forming the variances and spectra of amplitude and phase fluctuation of RO signal in the stratosphere and upper troposphere, at altitudes above 4–5 km in middle and polar latitudes, and above 7–8 km in the tropics. Simple relationships that link IGW parameters and RO signal fluctuations may serve as a basis for the global monitoring of IGW parameters and activity from RO amplitude and phase observations in the stratosphere and upper troposphere.

*Code availability.* The code used in this study does not belong to the public domain and cannot be distributed.

*Data availability.* GPS/MET radio occultation data are freely available. To get access to them, it is necessary to sign up at the website of the CDAAC: http://cdaac-www.cosmic.ucar.edu/cdaac/ (follow the "Sign up" link for further details).

*Competing interests.* The authors declare that they have no conflicts of interest.

*Acknowledgements.* The work of V. Kan and M. E. Gorbunov was supported by Russian Foundation for Basic Research, grant 16-05-00358.

## References

Alexandrov, A. P., Grechko, G. M., Gurvich, A. S., Kan, V., Manarov, M. K., Pakomov, A. I., Romanenko, Y. V., Savchenko, S. A., Serova, S. I., and Titov, V. G.: Spectra of temperature variations in the stratosphere as indicated by satellite–borne observation of the twinkling of stars, Izv. Atmos. Ocean. Phys., 26, 1–8, 1990.

Belloul, M. B. and Hauchecorne, A.: Effect of periodic horizontal gradients on the retrieval of atmospheric profiles from occultation measurements, Radio Science, 32, 469–478, 1997.

Bendat, J. S. and Piersol, A. G.: Random Data: Analysis and Measurement Procedures, J. Wiley, New York, 2nd edn., 1986.

Cornman, L. B., Frehlich, R., and Praskovskaya, E.: The detection of upper-level turbulence via GPS occultation methods, in: Occultations for Probing Atmosphere and Climate, edited by Kirchengast, P. D. G., Foelsche, D. U., and Steiner, D. A. K., Springer Verlag, 2004.

Cornman, L. B., Goodrich, R. K., Axelrad, P., and Barlow, E.: Progress in turbulence detection via GNSS occultation data, Atmos. Meas. Tech., 5, 789–808, doi:10.5194/amt-5-789-2012, 2012.

Cucurull, L.: Improvement in the Use of an Operational Constellation of GPS Radio Occultation Receivers in Weather Forecasting, Weather and Forecasting, 25, 749–767, 2010.

de la Torre, A., Schmidt, T., and Wickert, J.: A global analysis of wave potential energy in the lower stratosphere derived from 5 years of GPS radio occultation data with CHAMP, Geophys. Res. Lett., 33, L24 809, doi:10.1029/2006GL027696, 2006.

Eaton, F. D., Peterson, W. A., Hines, J. R., Peterman, K. R., Good, R. E., Beland, R. R., and Brown, J. H.: Comparison of VHF radar, optical, and temperature fluctuations measurements of $C_n^2$, $r_0$, and $\theta_0$, Theor. Appl. Climatol., 39, 17–29, 1988.

Ecklund, W. L., Carter, D. A., and Balsley, B. B.: Contiunuous measurements of upper atmospheric winds and turbulence using a VHF Doppler radar: Preliminary results, J. Atmos. Terr. Phys., 41, 983–994, 1979.

Fritts, D.: A review of gravity wave saturation processes, effects, and variability in the middle atmosphere, PAGEOPH, 130, 343–371, 1989.

Good, R. E., Watkins, B. J., Quesada, A. F., Brown, J. H., and Loriot, G. B.: Radar and Optical Measurements of $C_n^2$, Appl. Opt., 21, 3373–3376, 1982.

Gorbunov, M. E.: Ionospheric correction and statistical optimization of radio occultation data, Radio Sci., 37, 17–1–17–9, doi:10.1029/2000RS002370, 2002.

Gorbunov, M. E. and Lauritsen, K. B.: Analysis of Wave Fields by Fourier Integral Operators and its Application for Radio Occultations, Radio Sci., 39, RS4010, doi:10.1029/2003RS002971, 2004.

Gorbunov, M. E. and Lauritsen, K. B.: Radio Holographic Filtering of Noisy Radio Occultations, in: Atmosphere and Climate Studies by Occultation Methods, edited by Foelsche, U., Kirchengast, G., and Steiner, A., Springer, Berlin, Heidelberg, New York, 2006.

Gorbunov, M. E., Lauritsen, K. B., Rodin, A., Tomassini, M., and Kornblueh, L.: Analysis of the CHAMP Experimental Data on Radio-Occultation Sounding of the Earth's Atmosphere, Izvestiya, Atmospheric and Oceanic Physics, 41, 726–740, 2005.

Gracheva, M. E. and Gurvich, A. S.: A simple model for calculation of turbulence disturbances in optical devices, Izv. Akad. Nauk SSSR, Fiz. Atmos. Okeana, 16, 1107–1111, in Russian, 1980.

Gubenko, V. N., Pavelyev, A. G., and Andreev, V. E.: Determination of the Intrinsic Frequency and Other Wave Parameters from a Single Vertical Temperature or Density Profile Measurement, Journal of Geophysical Research, 113, D08 109, doi:10.1029/2007JD008920, 2008.

Gubenko, V. N., Pavelyev, A. G., Salimzyanov, R. R., and Pavelyev, A. A.: Reconstruction of internal gravity wave parameters from radio occultation retrievals of vertical temperature profiles in the Earth's atmosphere, Atmos. Meas. Tech., 4, 2153–2162, doi:10.5194/amt-4-2153-2011, 2011.

Gurvich, A. S.: Fluctuations During Observations of Extraterrestrial Sources from Space Through the Atmosphere of the Earth, Radiophysics and Quantum Electronics, 27, 665, 1984.

Gurvich, A. S. and Brekhovskikh, V. L.: Study of the Turbulence and Inner Waves in the Stratosphere Based on the Observations of Stellar Scintillations from Space: A Model of Scintillation Spectra, Waves in Random Media, 11, 163–181, 2001.

Gurvich, A. S. and Kan, V.: Structure of air density irregularities in the stratosphere from spacecraft observations of stellar scintillation: 1. Three-dimensional spectrum model and recovery of its parameters, Izv. Atmos. Ocean. Phys., 39, 300–310, 2003a.

Gurvich, A. S. and Kan, V.: Structure of air density irregularities in the stratosphere from spacecraft observations of stellar scintillation: 2. Characteristic scales, structure characteristics, and kinetic energy dissipation, Izv. Atmos. Ocean. Phys., 39, 311–321, 2003b.

Gurvich, A. S., Kon, A. I., Mironov, V. L., and Khmelevtsov, S. S.: Laser Radiation in the Turbulent Atmosphere, Nauka, Moscow, in Russian, 1976.

Gurvich, A. S., Kan, V., and Fedorova, O. V.: Stratospheric radio occultation measurements on the GPS-Microlab-1 satellite system: Phase fluctuations, Izvestiya, Atmospheric and Oceanic Physics, 36, 300–307, 2000.

Gurvich, A. S., Kan, V., Savchenko, S. A., Pakhomov, A. I., Borovikhin, P. A., Volkov, O. N., Kalery, A. Y., Avdeev, S. V., Korzun, V. G., Padalka, V. G., , and Podvyaznyi, Y. P.: Studying the turbulence and internal waves in the stratosphere from spacecraft observations of stellar scintillation: I. Experimental technique and analysis of the scintillation variance, Izv. Atm. Ocean. Phys., 37, 436–451, 2001a.

Gurvich, A. S., Kan, V., Savchenko, S. A., Pakhomov, A. I., and Padalka, V. G.: Studying the turbulence and internal waves in the stratosphere from spacecraft observations of stellar scintillation: 2. Probability distribution and spectra of scintillations, Izv. Atm. Ocean. Phys., 37, 452–465, 2001b.

Gurvich, A. S., Gorbunov, M. E., and Kornblueh, L.: Comparison Between Refraction Angles Measured in the Microlab-1 Experiment and Calculated on the Basis of an Atmospheric General Circulation Model, Izvestiya, Atmospheric and Oceanic Physics, 42, 709–714, 2006.

Hedin, A. E.: Extension of MSIS thermosphere model into the middle and lower atmosphere, J. Geophys. Res., 96, 1159–1172, 1991.

Hubbard, W. B., Jokipii, J. R., and Wilking, B. A.: Stellar occultation by turbulent planetary atmospheres: a wave-optical theory including a finite scale height, Icarus, 34, 374–395.

Hubbard, W. B., Lellouch, E., and Sicardy, B.: Structure of Scintillations in Neptune's Occultation Shadow, Astron. J., 325, 490–502, 1988.

Ishimaru, A.: Wave Propagation and Scattering in Random Media. Vol 2, Academic, New York, 1978.

Kan, V.: Coherence and correlation of chromatic stellar scintillations in a space-borne occultation experiment, Izv. Atmos. Ocean. Opt., 17, 725–735, 2004.

Kan, V., Matyugov, S. S., and Yakovlev, O. I.: The Structure of Stratospheric Irregularities According to Radio-Occultation Data Obtained Using Satellite-to-Satellite Paths, Izvestiya VUZov, Radiofizika, XLV, 652–663, 2002.

Kan, V., Sofieva, V. F., and Dalaudier, F.: Anisotropy of small-scale stratospheric irregularities retrieved from scintillations of a double star $\alpha$-Cru observed by GOMOS/ENVISAT, Atmos. Meas. Tech., 5, 2713–2722, doi:10.5194/amt-5-2713-2012, 2012.

Kan, V., Sofieva, V. F., and Dalaudier, F.: Variable anisotropy of small-scale stratospheric irregularities retrieved from stellar scintillation measurements by GOMOS/ENVISAT, Atmos. Meas. Tech., 7, 1861–1872, doi:10.5194/amt-7-1861-2014, 2014.

Khaykin, S. M., Hauchecorne, A., Mzé, N., and Keckhut, P.: Seasonal variation of gravity wave activity at midlatitudes from 7 years of COSMIC GPS and Rayleigh lidar temperature observations, Geophys. Res. Lett., 42, 1251–1258, doi:10.1002/2014GL062891, 2015.

McDonald, A. J.: Gravity wave occurrence statistics derived from paired COSMIC/FORMOSAT3 observations, J. Geophys. Res., 117, D15 406, doi:10.1029/2011JD016715, 2012.

Monin, A. S. and Yaglom, A. M.: Statistical Fluid Mechanics, Volume 2, MIT Press, Cambridge, Massachusetts, 1975.

Nastrom, G. D., Gage, K. S., and Ecklund, W. L.: Variability of Turbulence, 4–20 km, in Colorado and Alaska from MST Radar Observations, J. Geophys. Res., 91, 6722–6734, 1986.

Pingel, D. and Rhodin, A.: Assimilation of Radio Occultation Data in the Global Meteorological Model GME of the German Weather Service, in: New Horizons in Occultation Research, edited by Steiner, A., Pirscher, B., Foelsche, U., and Kirchengast, G., pp. 109–128, Springer, Berlin, Heidelberg, 2009.

Poli, P., Moll, P., Puech, D., Rabier, F., and Healy, S. B.: Quality Control, Error Analysis, and Impact Assessment of FORMOSAT-3/COS MIC in Numerical Weather Prediction, Terr. Atmos. Ocean. Sci., 20, 101–113, 2009.

Poli, P., Healy, S. B., and Dee, D. P.: Assimilation of Global Positioning System Radio Occultation Data in the ECMWF ERA-Interim Reanalysis, Q. J. R. Meteorol. Soc., 136, 1972–1990, doi:10.1002/qj.722, 2010.

Rennie, M. P.: The Impact of GPS Radio Occultation Assimilation at the Met Office, Quarterly Journal of the Royal Meteorological Society, 136, 116–131, doi:10.1002/qj.521, 2010.

Rocken, C., Kuo, Y.-H., Schreiner, W. S., Hunt, D., Sokolovskiy, S., and McCormick, C.: COSMIC System Description, Terrestrial, Atmospheric and Oceanic Science, 11, 21–52, 2000.

Rytov, S. M., Kravtsov, Y. A., and Tatarskii, V.: Principles of Statistical Radiophysics Vol 3, Springer-Verlag, 1989a.

Rytov, S. M., Kravtsov, Y. A., and Tatarskii, V.: Principles of Statistical Radiophysics : Wave Propagation Through Random Media Vol 4, Springer-Verlag, 1989b.

Shume, E. and Ao, C.: Remote sensing of tropospheric turbulence using GPS radio occultation, Atmos. Meas. Tech., 9, 3175–3182, 2016.

Smith, S. A., Fritts, D. C., and VanZandt, T. E.: Evidence of saturation spectrum of atmospheric gravity waves, J. Atmos. Sci., 44, 1404–1410, 1987.

Sofieva, V. F., Gurvich, A. S., Dalaudier, F., and Kan, V.: Reconstruction of internal gravity wave and turbulence parameters in the stratosphere using GOMOS scintillation measurements, J. Geophys. Res., 112, D12 113, doi:10.1029/2006JD007483, 2007a.

Sofieva, V. F., Kyrölä, E., Hassinen, S., Backman, L., Tamminen, J., Seppälä, A., Thölix, L., Gurvich, A. S., Kan, V., Dalaudier, F., Hauchecorne, A., Bertaux, J.-L., Fussen, D., Vanhellemont, F., D'Andon, O. F., Barrot, G., Mangin, A., Guirlet, M., Fehr, T., Snoeij, P., Saavedra, L., Koopman, R., and Fraisse, R.: Global analysis of scintillation variance: Indication of gravity wave breaking in the polar winter upper stratosphere, Geophys. Res. Lett., 34, L03 812, doi:10.1029/2006GL028132, 2007b.

Sofieva, V. F., Gurvich, A. S., and Dalaudier, F.: Gravity wave spectra parameters in 2003 retrieved from stellar scintillation measurements by GOMOS, Geophys. Res. Lett., 2009.

Sokolovskiy, S. V.: Modeling and Inverting Radio Occultation Signals in the Moist Troposphere, Radio Sci., 36, 441–458, 2001.

Steiner, A. K. and Kirchengast, G.: Gravity Wave Spectra from GPS/MET Occultation Observations, Journal of Atmospheric and Oceanic Technology, 17, 495–503, 2000.

Steiner, A. K., Kirchengast, G., Foelsche, U., Kornblueh, L., Manzini, E., and Bengtsson, L.: GNSS Occultation Sounding for Climate Monitoring, Phys. Chem. Earth (A), 26, 113–124, 2001.

Tatarskii, V. I.: The effects of the turbulent atmosphere on wave propagation, Translated from the Russian by the Israel Program for Scientific Translations, Jerusalem, 1971.

Tsuda, T., VanZandt, T. E., Mizumoto, M., Kato, S., and Fukao, S.: Spectral analysis of temperature and Brunt-Vaisala frequency fluctuations observed by radiosondes, J. Geophys. Res., 96, 17 265–17 278, 1991.

Tsuda, T., Nishida, M., Rocken, C., and Ware, R. H.: A global morphology of gravity wave activity in the stratosphere revealed by the GPS occultation data (GPS/MET), J. Geophys. Res., 105, 7257–7273, 2000.

Vorob'ev, V. V. and Krasil'nikova, T. G.: An approximate method for evaluation of refractive index variations in inhomogeneous atmosphere, Soviet Journal of Communications Technology and Electronics, 29, 199–206, in Russian, 1984.

Vorob'ev, V. V. and Krasil'nikova, T. G.: Estimation of the Accuracy of the Atmospheric Refractive Index Recovery from Doppler Shift Measurements at Frequencies Used in the NAVSTAR System, Izvestiya Academy of Sciences SSSR, Atmospheric and Oceanic Physics, English Translation, 29, 602–609, 1994.

Wang, L. and Alexander, M. J.: Global estimates of gravity wave parameters from GPS radio occultation temperature data, J. Geophys. Res., 115, D21 122, doi:10.1029/2010JD013860, 2010.

Ware, R., Exner, M., Feng, D., Gorbunov, M., Hardy, K., Herman, B., Kuo, Y.-H., Meehan, T., Melbourne, W., Rocken, C., Schreiner, W., Sokolovsky, S., Solheim, F., Zou, X., Anthes, R., Businger, S., and Trenberth, K.: GPS Sounding of the Atmosphere from Low Earth Orbit: Preliminary Results, Bulletin of the American Meteorological Society, 77, 19–40, 1996.

Wheelon, A.: Electromagnetic Scintillation. I. Geometrical optics, Cambridge University Press, Cambridge, UK, 2004.

Woo, R., Ishimaru, A., and Yang, F.-C.: Radio scintillations during occultations by turbulent atmospheres, Radio Sci., 15, 695–703, 1980.

Yakovlev, O. I., Efimov, A. I., Timofeeva, T. S., and Shvachkin, K. M.: Decimeter radio-wave fluctuations and energy flux during descent of the Venera 7 and Venera 8 probes to the surface of Venus, Cosmic Res. (USSR), 12, 100–103, 1974.

Yunck, T., Liu, C., and Ware, R.: A History of GPS Sounding, Terrestrial, Atmospheric and Oceanic Sciences, 11, 1–20, 2000.